Amino Acids (2015) 47:291–301
DOI 10.1007/s00726-014-1858-0

ORIGINAL ARTICLE

Directing peptide conformation with centrally positioned pre-organized dipeptide segments: studies of a 12-residue helix and β-hairpin

Siddappa Chandrappa · M. B. Madhusudana Reddy · Rajesh Sonti · Krishnayan Basuroy · Srinivasarao Raghothama · Padmanabhan Balaram

Received: 18 August 2014 / Accepted: 14 October 2014 / Published online: 16 November 2014

Abstract Secondary structure formation in oligopeptides can be induced by short nucleating segments with a high propensity to form hydrogen bonded turn conformations. Type I/III turns facilitate helical folding while type II′/I′ turns favour hairpin formation. This principle is experimentally verified by studies of two designed dodecapeptides, Boc-Val-Phe-Leu-Phe-Val-**Aib-Aib**-Val-Phe-Leu-Phe-Val-OMe **1** and Boc-Val-Phe-Leu-Phe-Val-**^{D}Pro-^{L}Pro**-Val-Phe-Leu-Phe-Val-OMe **2**. The N- and C-terminal flanking pentapeptide sequences in both cases are identical. Peptide **1** adopts a largely α-helical conformation in crystals, with a small 3_{10} helical segment at the N-terminus. The overall helical fold is maintained in methanol solution as evidenced by NMR studies. Peptide **2** adopts an antiparallel β-hairpin conformation stabilized by 6 interstrand hydrogen bonds. Key nuclear Overhauser effects (NOEs) provide evidence for the antiparallel β-hairpin structure. Aromatic proton chemical shifts provide a clear distinction between the conformation of peptides **1** (helical) and **2** (β-hairpin). The proximity of facing aromatic residues positioned at non-hydrogen bonding positions in the hairpin results in extensively ring current shifted proton resonances in peptide **2**.

Electronic supplementary material The online version of this article (doi:10.1007/s00726-014-1858-0) contains supplementary material, which is available to authorized users.

S. Chandrappa · M. B. Madhusudana Reddy · R. Sonti · K. Basuroy · P. Balaram (✉)
Molecular Biophysics Unit, Indian Institute of Science, Bangalore 560012, India
e-mail: pb@mbu.iisc.ernet.in

S. Raghothama
Sophisticated Instrumentation Facility, Indian Institute of Science, Bangalore 560012, India

Keywords α-Helix · β-Hairpin · Peptide conformation · Aromatic residues

Introduction

Peptide design strategies aimed at constructing well-designed secondary structures in synthetic oligopeptides have often used strategically placed, conformationally constrained residues to induce the formation of local folding nuclei. Helix induction by the incorporation of α,α dialkylated residues, most notably α-aminoisobutyric acid (Aib) and hairpin nucleation by centrally positioned ^{D}Pro-Xxx segments have been extensively investigated (Venkatraman et al. 2001; Aravinda et al. 2013a, b). These approaches rely on the very high propensity of Aib-Xxx/Xxx-Aib and ^{D}Pro-Xxx peptide segments to form $4 \rightarrow 1$ hydrogen bonded β-turn conformations. The Aib residue strongly favours backbone conformations in the 3_{10} helical regions of ϕ ($\approx\pm60°$), ψ ($\approx\pm30°$) space, promoting formation of type I/III β-turn, when Xxx is an L-residue (Benedetti et al. 1982; Toniolo et al. 1983; Prasad and Balaram 1984; Karle and Balaram 1990; Crisma et al. 2006). A continuous repetition of successive type III turns along a polypeptide segment generates a 3_{10} helical structure (Toniolo and Benedetti 1991). The ^{D}Pro-Xxx dipeptide segment strongly favours formation of type II´ β-turns, when Xxx is an L-residue ϕ_{i+1}, ψ_{i+1}($\approx60°$, $\approx-120°$) ϕ_{i+2}, ψ_{i+2} ($\approx-80°$, $\approx0°$) (Venkatraman et al. 2001). When prime turns, type I´/II´, are centrally positioned in an oligopeptide sequence, hairpin formation with two registered antiparallel strands is facilitated (Awasthi et al. 1995; Karle et al. 1996; Haque et al. 1996; Gellman 1998).

In ongoing studies on the design of structured peptides, we have investigated the effects of centrally positioned

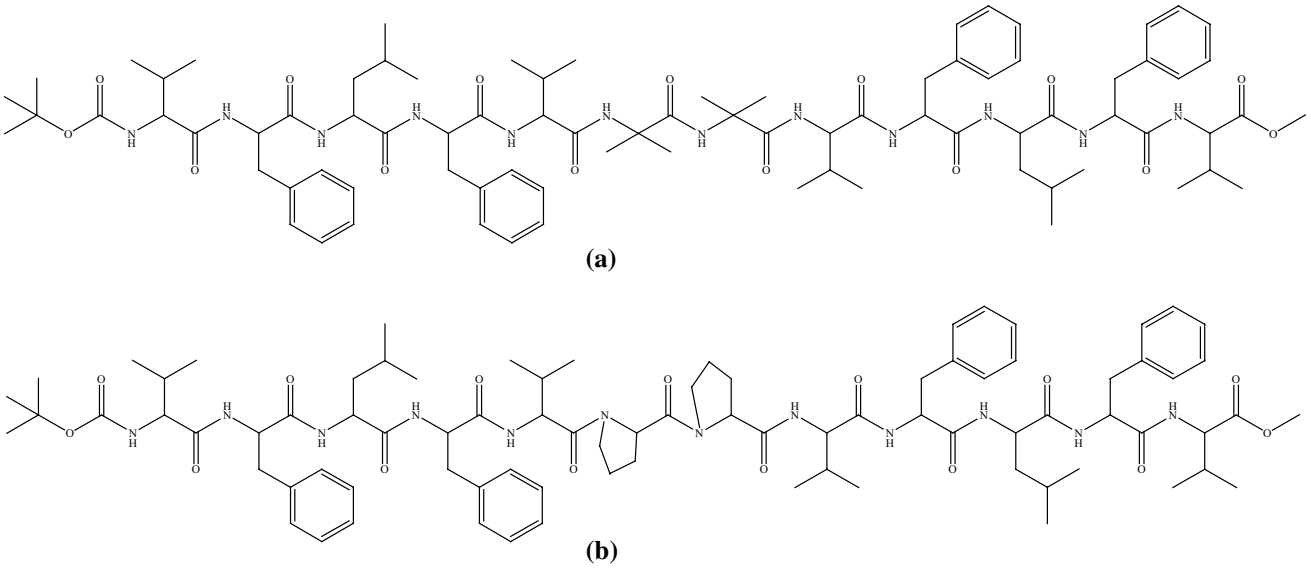

Fig. 1 Chemical structure of the dodecapeptides studied. **a** Boc-Val-Phe-Leu-Phe-Val-**Aib-Aib**-Val-Phe-Leu-Phe-Val-OMe **1**. **b** Boc-Val-Phe-Leu-Phe-Val-**^{D}Pro-^{L}Pro**-Val-Phe-Leu-Phe-Val-OMe **2**

Aib-Aib (U-U) and ^{D}Pro-^{L}Pro (^{D}P-^{L}P) segments on the conformation of identical flanking pentapeptide segments. The model 12 residue peptides investigated are Boc-Val-Phe-Leu-Phe-Val-**Aib-Aib**-Val-Phe-Leu-Phe-Val-OMe **1** and Boc-Val-Phe-Leu-Phe-Val-**^{D}Pro-^{L}Pro**-Val-Phe-Leu-Phe-Val-OMe **2** (Fig. 1). Previous studies have established a strong tendency of ^{D}Pro-^{L}Pro segments to promote type II' β-turn formation facilitating hairpin formation (Robinson 2000, 2008; Rai et al. 2006; Aravinda et al. 2013a, b). Indeed, the ^{D}P–^{L}P unit has been effectively used in the engineering of structured peptides for diverse applications, ranging from design of immunogenic peptides (Riedel et al. 2011; Robinson 2013; Schmidt et al. 2013) to the formation of peptide hydrogels for controlled drug delivery (Rughani and Schneider 2008; Rajagopal et al. 2009; Gungormus et al. 2010; Altunbas et al. 2011; Veiga et al. 2012). The achiral Aib-Aib segment can, in principle, adopt type I/III or I'/III' β-turn conformations. When placed at the centre of a 12-residue segment in which flanking pentapeptides are composed of all L-amino acids, the **Aib-Aib** unit could, in principle, facilitate both helical and hairpin structures depending on the local conformations selected at the central dipeptide (Rai et al. 2007; Rajagopal et al. 2011). For a 12-residue peptide sequence, a continuous 3_{10}-helical conformation supports the formation of 10 intramolecular 4 → 1 hydrogen bonds, whereas a perfectly registered hairpin would contain 6 inter-strand hydrogen bonds. The results reported herein are based on studies in methanol solution, where solvent solute hydrogen bonding may be expected to compensate for the differences in the energetic contributions of the intramolecular hydrogen bonds in the two distinct structures. The positions of the four phenylalanine residues [(Phe(2), Phe(4), Phe(9) and Phe(11)] were specifically chosen in order to probe hairpin formation using aromatic ring current induced upfield shifts of Phe ring protons, when residues occur on facing strands at non-hydrogen bonding positions. Previous studies have established that proximal disposition of aromatic residues at facing cross-strand positions result in large chemical shift perturbations, which can then serve as a diagnostic for hairpin conformations (Rajagopal et al. 2012; Sonti et al. 2012, 2013). The studies detailed in this report establish a continuous helical conformation in peptide **1** (Aib-Aib) both in crystals and in solution, while a β-hairpin is established in solution for peptide **2** (^{D}Pro-^{L}Pro). The results demonstrate conformational plasticity of the flanking N and C-terminus pentapeptide segments, which switch between helical and β-strand conformations under the influence of the central β-turn dipeptide segment.

Results and discussion

Conformations of **1** in methanol solution

NMR studies of peptides **1** and **2** were carried out in methanol solution at 500 MHz. Both peptides yielded well-resolved ^{1}H NMR spectra, permitting straightforward sequence-specific assignment of resonances, using a combination of TOCSY and ROESY experiments. Temperature dependence of NH chemical shifts, backbone $^{3}J_{NH-C^{\alpha}H}$ and Phe side chain coupling constants, $^{3}J_{C^{\alpha}H-C^{\beta}H}$ were determined. Relevant NMR parameters for peptides **1** and **2** are

Table 1 NMR parameters for peptide Boc-Val-Phe-Leu-Phe-Val-**Aib–Aib**-Val-Phe-Leu-Phe-Val-OMe **1** and Boc-Val-Phe-Leu-Phe-Val-**^{D}Pro-^{L}Pro-**Val-Phe-Leu-Phe-Val-OMe **2** in CD_3OH solution

Residue	NH		$C^{\alpha}H$		dδ/d*t* (ppb/K)		$^{3}J_{NH-C^{\alpha}H}$ (Hz)		$^{3}J_{C^{\alpha}H-C^{\beta}H}$ (Hz)	
	1	**2**	**1**	**2**	**1**	**2**	**1**	**2**	**1**	**2**
Val(1)	7.03	6.14	3.81	3.98	6.30	2.00	3.10	9.70		
Phe(2)	8.27	8.11	4.39	5.32	11.00	11.00	2.90	–	7.80, 7.10	11.00, 5.40
Leu(3)	7.77	8.81	4.07	4.71	4.20	5.00	6.20	9.10		
Phe(4)	7.43	8.61	4.34	5.30	3.20	12.00	6.70	–	5.30, 10.30	9.20, 4.50
Val(5)	7.58	8.96	3.68	4.48	5.20	4.00	6.50	9.80		
Aib(6)/^{D}Pro(6)	7.96	–	–	4.68	5.50	–	–	–		
Aib(7)/^{L}Pro(7)	7.61	–	–	4.60	3.20	–	–	–		
Val(8)	7.64	7.84	3.75	4.22	2.20	1.20	5.50	9.20		
Phe(9)	7.88	8.12	4.45	5.18	3.20	7.50	6.00	9.20	3.00, 11.00	7.60, 6.30
Leu(10)	7.86	8.74	4.30	4.66	3.50	3.50	7.70	9.30		
Phe(11)	7.78	8.53	4.63	4.84	4.50	9.00	7.10	7.80	4.50, 9.80	10.00, 3.60
Val(12)	7.80	8.22	4.28	4.13	5.00	6.00	6.60	9.40		

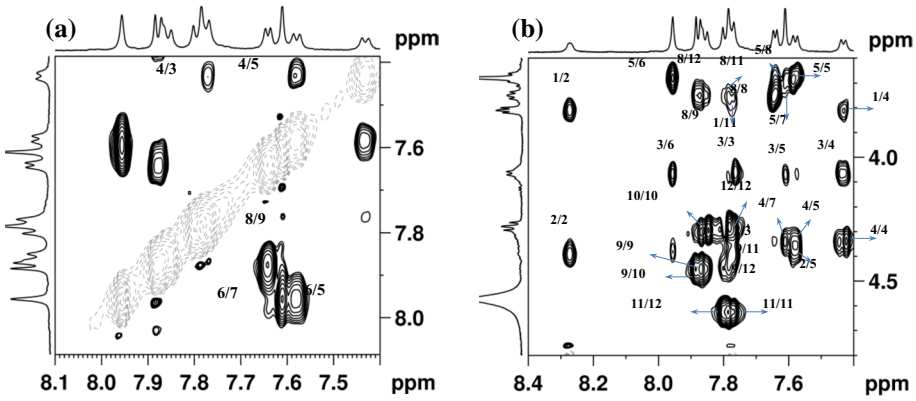

Fig. 2 Peptide **1**: partial ROESY spectra highlighting **a** NH↔NH (d_{NN}) and **b** $C^{\alpha}H$↔NH ($d_{\alpha N}$) NOEs

listed in Table 1 (see also supplementary Figs. S1 and S2 for NMR spectra and Table S1 for a complete listing of proton chemical shifts). A notable feature of the spectrum of peptide **1** is significant broadening of the Val(1) and Phe(2) NH resonances, suggestive of an exchange process at 303 K. These resonances *sharpen* upon cooling over the temperature range 313–283 K, suggestive of a slower rate of exchange with solvent protons. Interestingly, broadening of the N-terminus NH resonances Val(1), Phe(2), Leu(3) and Phe(4) is also observed in peptide **2**, with the important difference that in this case the resonances *broaden* upon cooling, over the temperature range 313–273 K. These observations are indicative of exchange processes involving conformational fluctuations or solvent exchange involving the N-terminus segments of both peptides.

Figure 2 shows partial ROESY spectra, illustrating the NOEs that serve as diagnostics for the secondary structure adopted by peptide **1**. In peptide **1** (Aib-Aib) sequential d_{NN} ($NH_i \leftrightarrow NH_{i+1}$) NOEs are observed for residues 3–9, suggestive of a continuous helical conformation over the central segment of the peptide. Additional backbone NOEs of the type $d_{\alpha N}(i, i+1)$ $(i, i+2)$ $(i, i+3)$ are also observed. These NOEs are consistent with a helical conformation over the segment, residues 1–8. The d_{NN} NOEs corresponding to the C-terminus segment, residues 9–11, are not observed because of limited chemical shift dispersion of these resonances. The observed NOEs support a continuous helical conformation for peptide **1**. Inspection of the temperature coefficients (dδ/d*T*) of NH resonances in CD_3OH (Table 1) provides further evidence for helical conformations. While Val(1) NH and Phe(2) NH exhibit dδ/d*T* values greater than 6 ppb/K, the remaining 10 NH resonances yield values between 2.2 and 5.5 ppb/K The observed $^{3}J_{NH-C^{\alpha}H}$ values are also consistent with ϕ values of $-60°$, which are anticipated in a helical conformation. The NMR evidence thus suggests an overall helical fold for peptide **1**, with a degree of flexibility at the N- and C-termini.

Molecular conformation of peptide **1** in crystals

X-ray diffraction using single crystals readily obtained from methanol, yielded the helical conformation illustrated

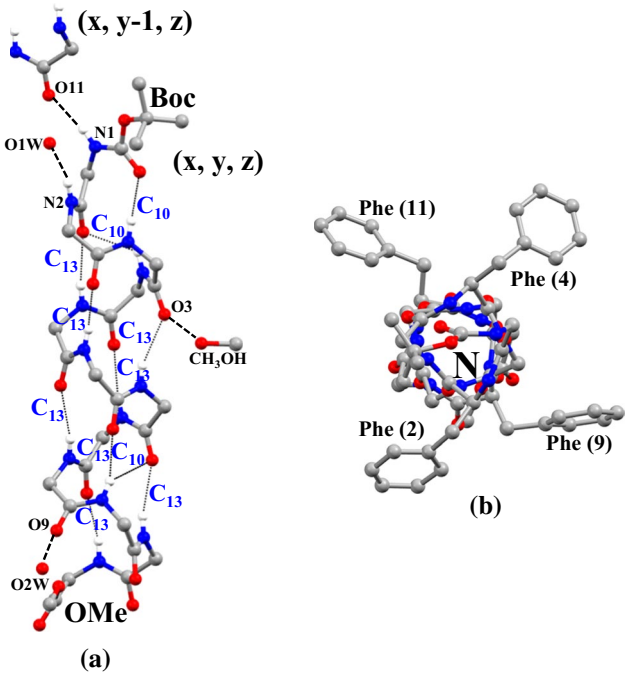

Fig. 3 Peptide **1**: **a** molecular conformation in crystals and immediate intermolecular interactions of the peptide molecule. **b** A projection down the helix axis, showing the disposition of four Phe sidechains (the projection is from N to C terminus)

Table 2 Crystal data and structure refinement parameters of peptide Boc-Val-Phe-Leu-Phe-Val-**Aib-Aib**-Val-Phe-Leu-Phe-Val-OMe **1**

Empirical formula	$C_{82}H_{120}N_{12}O_{15} + 2H_2O + 4CH_3OH$
Crystal habit [crystal size (mm)]	Rectangular block (0.34 × 0.22 × 0.10)
Crystallizing solvent	Methanol/water
Space group	$P2_12_12_1$
a (Å)	18.445(1)
b (Å)	21.2992(9)
c (Å)	24.495(1)
Volume (Å^3)	9,623.4(8)
Z/Z′	4/1
Co-crystallized solvent	2O (H_2O) +4CO(CH_3OH)
Molecular weight, calculated density (g/cm^3)	1,657.94, 1.144
F (000)	3,552
Radiation	Mo K_α (0.71073 Å)
Temperature (K)	220
2θ max. (°)	60.30
Unique reflections (measured reflections)	15,033 (105,890)
Observed reflection [$\lvert F \rvert > 4\sigma(F)$]	9,673
R_{int}	0.0551
Final *R* (%)/*w*R2 (%)	9.94/30.51
Goodness-of-fit on F^2 (*S*)	1.049
$\Delta\rho$ max (e.Å^{-3})/$\Delta\rho$ min(e.Å^{-3})	0.74/−0.41
No. of restraints/parameters	269/1,089
Data [$\lvert F \rvert > 4\sigma(F)$]-to-parameter ratio	8.88:1

in Fig. 3. Table 2 lists the crystal data and structure refinement parameters of peptide **1**. Backbone torsion angles and intramolecular hydrogen bond parameters are summarized in Tables 3 and 4. The Ramachandran angles (ϕ, ψ) lie within the $3_{10}/\alpha_R$ regions with a moderate deviation observed for the Phe(9) residue (Table 3). From Tables 3 and 4 it is evident that the molecule adopts a largely right handed α-helical conformation (5 → 1 hydrogen bonds), with a small segment of 3_{10}-helix (4 → 1 hydrogen bonds) at the N-terminus. A distinction between 3_{10} and α-helical conformation is often not possible on the basis of torsion angle values alone. Careful inspection of 4 → 1 and 5 → 1 hydrogen bond parameters is necessary in the case of helical peptides (Aravinda et al. 2004). Supplementary Table S2 provides a complete listing of all the relevant parameters for potential 4 → 1 and 5 → 1 hydrogen bonds. An interesting feature of the structure is the presence of as many as six molecules of solvent (2 H_2O + 4 CH_3OH) in the asymmetric unit, which contains a single peptide molecule. Solvent molecules which interact directly with backbone amide groups are shown in Fig. 3. The water molecules O1 and O2W form hydrogen bonds to the exposed N2H and CO9 groups which lie at the N- and C-terminus of the helix and do not participate in the intramolecular hydrogen bonds. Figure 4 shows the network of solvent interactions in the crystal structure of peptide **1**. The oxygen atom O2M of one of the co-crystallized methanol molecule forms hydrogen bonds to CO3 without disrupting the 5 → 1 hydrogen bond.

Conformations of peptide 2 in solution

A comparison of the backbone proton chemical shifts $C^\alpha H$, NH, dδ/dT values and $^3J_{NH-C^\alpha H}$ values for peptides **1** and **2** clearly suggests a dramatic difference in the conformations of the two peptides. The large values of $^3J_{NH-C^\alpha H}$ (>9 Hz) for all residues in peptide **2,** with the exception of Phe(11), strongly suggest extended β-strand conformation at both N- and C-terminal segments. The low field position of all $C^\alpha H$ resonances in peptide **2** relative to the corresponding resonances of residues in peptide **1**, with the exception of Val(12), are suggestive of a β-strand conformation over residues 1–5 and 8–11. In a β-hairpin conformation, with a central ^{D}Pro-^{L}Pro segment, 6 interstrand hydrogen bonds involving Val(1), Leu(3), Val(5), Val(8), Leu(10) and Val(12) are anticipated (Fig. 5a). The NH groups of

Phe(2), Phe(4), Phe(9) and Phe(11) are exposed to solvent. The dδ/dT values listed in Table 1 indeed establish significantly higher temperature coefficients for Phe(2), Phe(4), Phe(9) and Phe(11) NH groups, while low temperature coefficients are obtained for Val(1), Val(5), Val(8) and Leu(10) NH groups. In the case of hairpins, cross-strand NOEs provide direct evidence for the folded conformation. Figure 6 illustrates the key NOEs which define the β-hairpin structure in peptide **2**. Using a total of 27 NOE restraints and 8 torsion angle restraints (supplementary Table S3), derived from $^{3}J_{NH-C^{\alpha}H}$ values, a structure calculation was carried out using the NMR module in INSIGHT II. Figure 5b shows the superposition of NMR-derived structures.

Table 3 Backbone torsion angles (°) in the crystal structure of peptide Boc-Val-Phe-Leu-Phe-Val-**Aib-Aib**-Val-Phe-Leu-Phe-Val-OMe **1**

Residues	ϕ	ψ	ω
Val(1)	−60.4	−19.4	171.0
Phe(2)	−45.3	−41.4	−177.4
Leu(3)	−61.9	−37.1	175.7
Phe(4)	−67.1	−46.4	177.7
Val(5)	−56.4	−51.1	−176.7
Aib(6)	−56.5	−49.7	−177.1
Aib(7)	−54.8	−50.1	−178.0
Val(8)	−56.9	−46.8	−174.9
Phe(9)	−82.6	−3.9	164.7
Leu(10)	−80.8	−46.3	−176.5
Phe(11)	−76.5	−37.4	169.6
Val(12)	−73.6	−35.2	174.2

Aromatic proton chemical shifts

A feature of the sequences of peptides **1** and **2** is the regular positioning of the four Phe residues. In an ideal hairpin conformation, all four Phe residues occur on the same face of the β-hairpin and cross-strand aromatic interactions may be anticipated between Phe(2)/Phe(11) and Phe(4)/Phe(9). Indeed, the proximity of the aromatic residues across antiparallel strands results in substantial upfield shifts for specific aromatic protons and has been used for the analysis of Phe ring orientations in designed β-sheet and three stranded β-sheet structures (Rajagopal et al. 2012; Sonti et al. 2012, 2013). Figure 7 compares the aromatic proton

Table 4 Hydrogen bonds in the crystal structure of peptide Boc-Val-Phe-Leu-Phe-Val-**Aib-Aib**-Val-Phe-Leu-Phe-Val-OMe **1**

Donor	Acceptor	D…A (Å)	H…A (Å)	D-H…A (°)	C=O…H (°)	C=O…D (°)
Intramolecular hydrogen bonds						
N3	O0 [**4** → **1** ($\mathbf{3_{10}}$)]	3.01	2.19	159.1	131.6	132.9
N4	O1 [**4** → **1** ($\mathbf{3_{10}}$)]	2.94	2.38	123.3	113.8	125.8
N5	O1 [**5** → **1** (α_R)]	3.07	2.22	169.1	158.5	161.3
N6	O2 [**5** → **1** (α_R)]	2.84	1.99	169.4	157.7	160.6
N7	O3 [**5** → **1** (α_R)]	3.09	2.27	160.1	137.5	142.8
N8	O4 [**5** → **1** (α_R)]	3.01	2.16	167.7	154.5	157.6
N9	O5 [**5** → **1** (α_R)]	3.08	2.25	161.4	156.3	160.6
N10	O6 [**5** → **1** (α_R)]	3.01	2.32	137.4	151.3	161.7
N10	O7 [**4** → **1** ($\mathbf{3_{10}}$)]	3.25	2.57	136.6	98.5	108.7
N11	O7 [**5** → **1** (α_R)]	3.19	2.34	166.3	156.7	159.4
N12	O8 [**5** → **1** (α_R)]	2.85	2.00	168.4	160.2	162.9
Intermolecular hydrogen bonds						
N1	O11 (x, $y-1$, z)	2.85	2.00	166.1	134.7	138.8
Solvent-mediated hydrogen bonds						
N2	O1W	2.94	2.10	164.9		
O1W	O10 (x, $y+1$, z)	3.08				156.6
O1M	O1W	2.82				
O2W	O9	2.20				159.9
O2W	O0 ($x+1/2$, $-y+1/2$, $-z$)	2.92				114.2
N4 ($x+1/2$, $-y+1/2$, $-z$)	O2W	3.16	2.47	138.3		
O1M	O4M ($-x+1$, $y-1/2$, $-z-1/2$)	2.81				
O2 M	O3	2.84				125.6
O3M	O2M	2.74				
O4M	O3M	2.77				

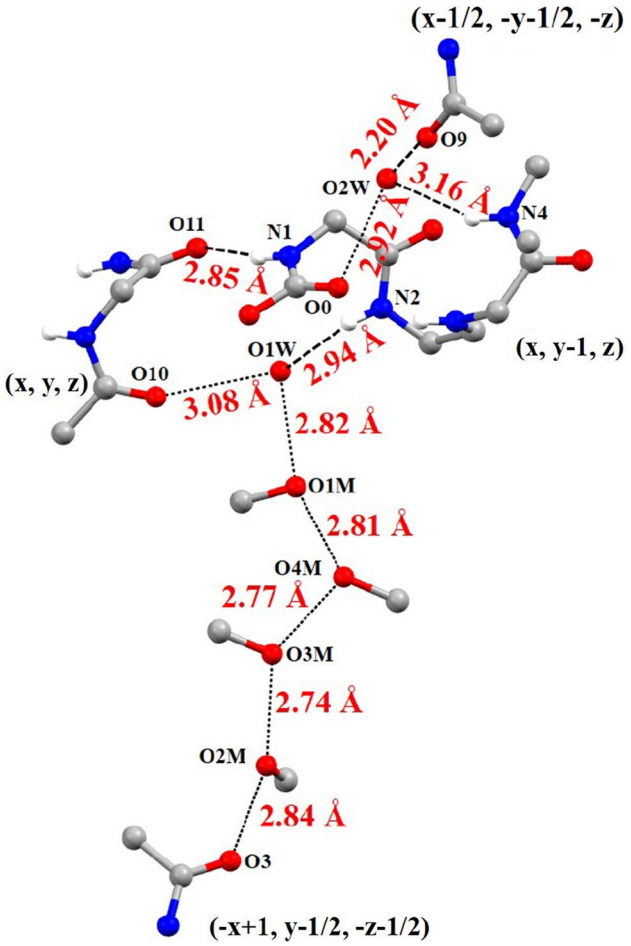

Fig. 4 Network of solvent interactions in the crystal structure of peptide Boc-VFLFV-UU-VFLFV-OMe **1**

resonances of the pentapeptide fragment Boc-VFLFV-OMe with those observed for helical peptide **1** and β-hairpin peptide **2**. It is immediately evident that a significantly greater dispersion of aromatic resonances is observed in the β-hairpin peptide **2** as compared to helical peptide **1** and the isolated pentapeptide. A noteworthy feature of the spectrum in Fig. 7 is that both these structured peptides show distinct shifts of aromatic resonances relative to the isolated pentapeptide fragment. Interestingly, small but nevertheless significant downfield shifts of specific aromatic resonances are noted in peptide **1**, while large upfield shifts are seen in peptide **2**. Specific assignment of aromatic resonances in peptides **1** and **2** facilitates further analysis. These assignments are readily achieved by using a combination of HSQC and HSQC-TOCSY experiments detailed earlier (Sonti et al. 2012, 2013). Figure 8 illustrates the relevant regions of the HSQC spectra of peptides **1** and **2**, which permit individual aromatic assignments. Table 5 summarizes aromatic proton chemical shifts for the four Phe residues in peptides **1** and **2**. The hairpin structure is characterized by large upfield shifts of the Phe(9) and Phe(11) $C^{\delta}H_2$ protons and Phe(9) $C^{\varepsilon}H_2/C^{\zeta}H$ protons. The Phe(4) $C^{\zeta}H$ proton is also significantly shifted to higher field. These observations provide further support for the close clustering of the aromatic rings in the β-hairpin conformations of the peptide **2**. A notable feature in the helical peptide **1** is the shift to low field of 7.35 ppm of the Phe(9) $C^{\delta}H_2$ proton resonances. Inspection of the disposition of the four Phe side chains in the crystal structure of peptide **1** (Fig. 3b) reveals that all four aromatic residues point away from each other. The downfield shift of the Phe(9) $C^{\delta}H_2$ resonance may be ascribed to diamagnetic anisotropy effects arising from the proximal amide group. The above results establish that the chemical shifts of these aromatic ring resonances establish a clear distinction between the two distinct secondary structures, helix and hairpin. Recent studies suggest cross-strand interactions between aromatic residues may indeed be a stabilizing feature in β-hairpins even in organic solvents (Sonti et al. 2012, 2013).

Conclusion

NMR and crystallographic studies summarized above establish that peptide **1** which contains a centrally positioned Aib-Aib residues favours a continuous helical conformation in both solid state and solution. In contrast, peptide **2** which contains a centrally positioned ^{D}Pro-^{L}Pro segment favours β-hairpin conformation stabilized by 6 interstrand hydrogen bonds. For both peptides, observed conformations have been determined in the same solvent, methanol. These results provide direct evidence for the role of nucleating segments, which facilitate the formation of local secondary structures. The pentapeptide segment, VFLFV, which contains three distinct hydrophobic amino acids, adopts two distinct conformations depending on the conformational propensities of the positioned, nucleating dipeptide. Conformational plasticity is a characteristic of amino acid sequences in the absence of locally constraining residues. In short peptides local conformational fluctuation at individual residues results in dynamic interconversions between ensembles of diverse structures. In proteins when tertiary interactions impose structural constraints, short peptide segments with identical sequences can be captured in distinct conformational states, when embedded in different polypeptide sequences. The model system described in this report establishes that dramatically different conformations can be induced by appropriate positioning of a locally constrained dipeptide segment. The precise conformational features of the nucleating segment then determine the structure induced in the flexible pentapeptide.

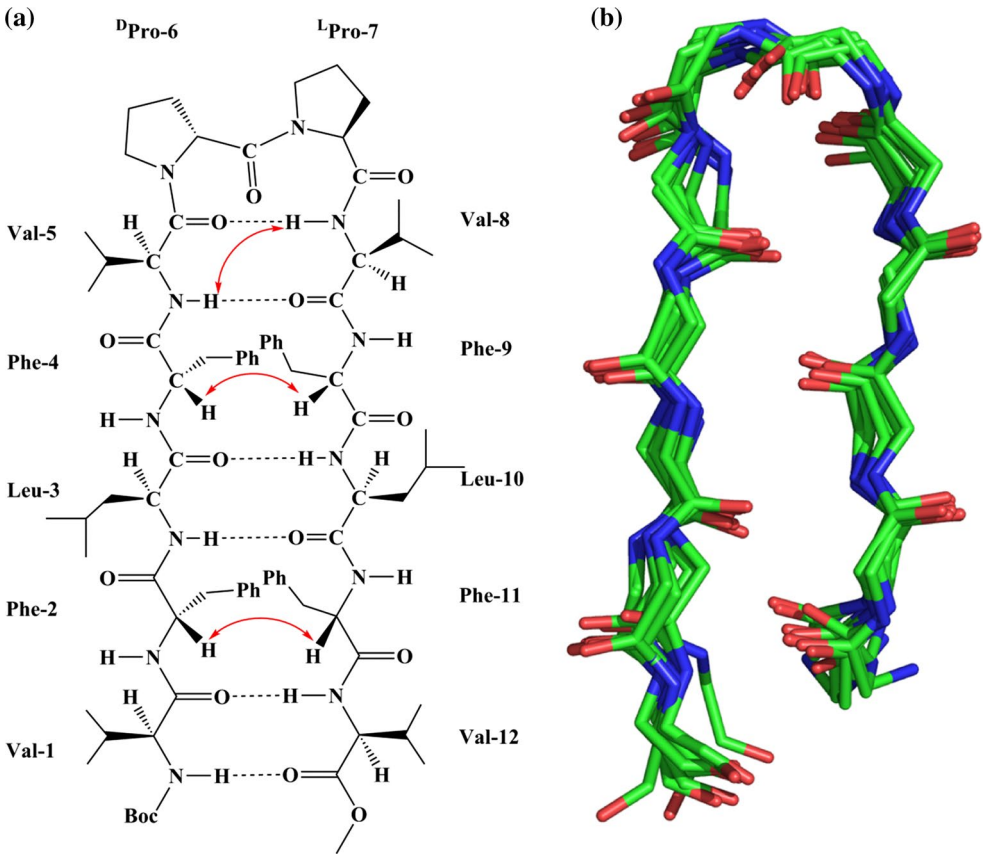

Fig. 5 **a** Schematic representation of peptide **2**. Expected hydrogen bonds are shown as broken lines and NH↔NH (d_{NN}) and $C^{\alpha}H \leftrightarrow C^{\alpha}H$ ($d_{\alpha\alpha}$) NOEs with curved arrow. **b** Superposition of the best structures calculated for peptide **2** using NOE constraints from the ROESY spectra in CD_3OH (10 best structures were superposed)

Experimental section

Peptide synthesis

Boc-Val-Phe-Leu-Phe-Val-**Aib-Aib**-Val-Phe-Leu-Phe-Val-OMe **1**, Boc-Val-Phe-Leu-Phe-Val-**^{D}Pro-^{L}Pro**-Val-Phe-Leu-Phe-Val-OMe **2** and Boc-Val-Phe-Leu-Phe-Val-OMe **3** were synthesized by classical solution phase methods by using a racemization-free fragment condensation strategy. The tert-butyloxycarbonyl (Boc) group was used to protect the N-terminus. Deprotections were performed using 98 % formic acid and saponification for the N- and C-terminal protection groups, respectively. Couplings were mediated by N,N′-dicyclohexylcarbodiimide (DCC) and 1-hydroxybenzotriazole (HOBt). All intermediates were characterized by ESI-MS and TLC on silica gel [$CHCl_3$/MeOH, 9:1 v/v)] and were used without further purification. The pentapeptide Boc-Val-Phe-Leu-Phe-Val-OMe **3** was synthesized by stepwise coupling of the dipeptide Boc-Phe-Val-OMe at the N-terminus. The Boc group was deprotected and the pentapeptide free base was coupled to the dipeptide and Boc-Aib-Aib-OH or Boc-^{D}Pro-^{L}Pro-OH. In the final steps, the heptapeptide free base was coupled to the pentapeptide acid in a 5+7 coupling using DCC/HOBt. The final peptides were purified by reversed-phase high-performance liquid chromatography (HPLC) on a Jupitor Proteo C12 column (10–250 mm, 4 μ particle size) using methanol/water systems and monitored at 226 nm. ESI-MS was performed with a Bruker Daltonics Esquire-3000 instrument, and ^{1}H NMR spectra were recorded with Bruker 500 or 700 MHz spectrometers. Mass spectral data (*m/z* in Da): Peptide **1**, 1515.1 $[M+H]^+$ (Mcal 1514.93); 1536.2 $[M+Na]^+$; 1552.2 $[M+K]^+$; **2**, 1538.2 $[M+H]^+$ (Mcal 1538.95); 1560.4 $[M+Na]^+$; 1576.5 $[M+K]^+$; **3**, 738.4 $[M+H]^+$ (Mcal 738.94); 760.4 $[M+Na]^+$; 776.4 $[M+K]^+$ (supplementary Figs. S4, S5, S6).

NMR spectroscopy

NMR spectra were recorded on Bruker Avance 500 MHz spectrometer. All NMR experiments were carried out in methanol solutions (CD_3OH). Intramolecular hydrogen bonding was probed by recording 1D spectra at five different temperatures ranging 273–313 K at 10-K intervals

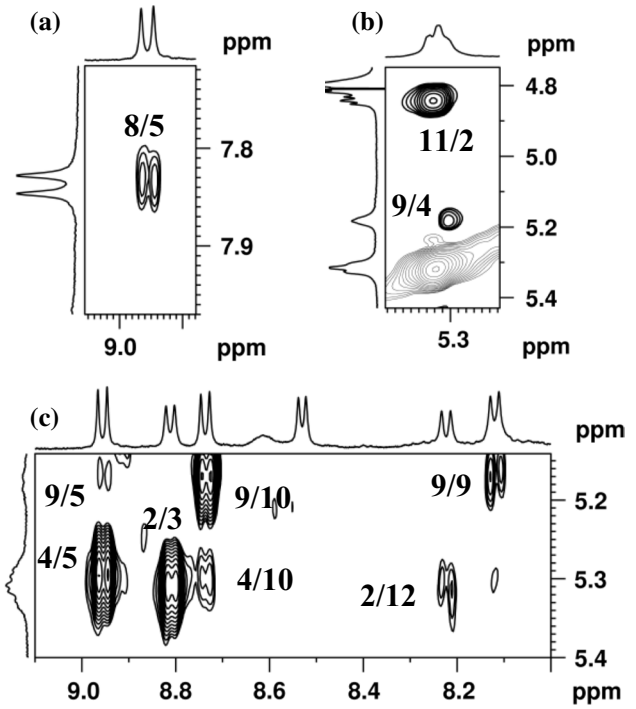

Fig. 6 Peptide **2**: partial ROESY spectra highlighting **a** NH↔NH (d_{NN}), **b** $C^{\alpha}H \leftrightarrow C^{\alpha}H$ ($d_{\alpha\alpha}$) and **c** $C^{\alpha}H \leftrightarrow NH$ ($d_{\alpha N}$) NOEs

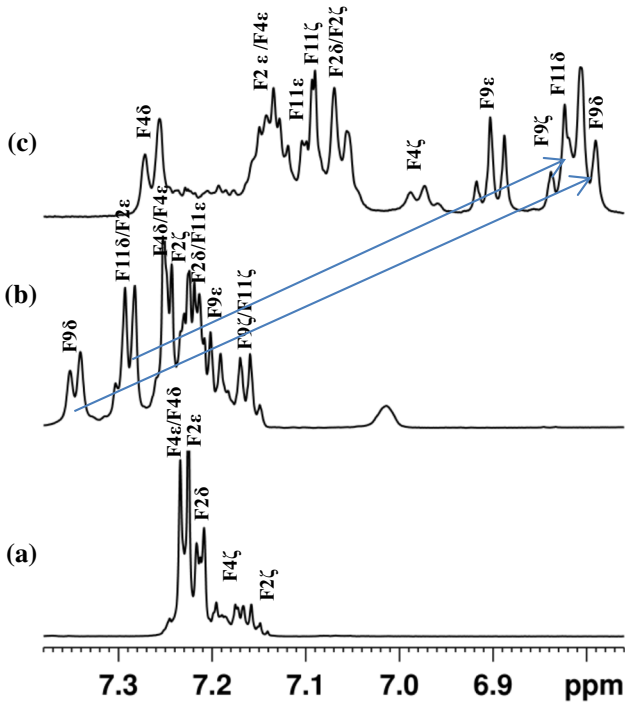

Fig. 7 Comparison of aromatic resonances of the pentapeptide fragment **a** Boc-VFLFV-OMe with those observed for, **b** helical peptide **1** and **c** β-hairpin peptide **2**

and determining the temperature coefficients of amide proton chemical shifts. Water suppression was carried out using an excitation sculpting pulse sequence (Hwang and Shaka 1995). Residue-specific assignments were obtained from TOCSY (Braunschweiler and Ernst 1983) experiments, while ROESY (Bothner-By et al. 1984) spectra were used for sequence-specific assignments. TOCSY and ROESY experiments were recorded with excitation sculpting embedded pulse sequences obtained from BRUKER library. Residue-specific, unambiguous aromatic proton chemical shifts were assigned by using a combination of 2D HSQC (Kay et al. 1992) and HSQC-TOCSY (Otting and Wüthrich 1988) experiments as illustrated previously. All 2D experiments were recorded in phase sensitive mode using STATES-TPPI for TOCSY and ROESY and Echo-Antiecho mode for HSQC and HSQC-TOCSY in the F1 dimension. A data set of 2,048 × 400 was used for acquiring the data. The same data set was zero filled to yield a data matrix of size 4,096 × 1,024 before Fourier transformation. A spectral width of 12 ppm was used in both dimensions for TOCSY and ROESY experiments. Mixing times of 80 ms for TOCSY, 50 and 200 ms for ROESY and 80 ms for HSQC-TOCSY were used. Shifted square sine bell windows were used while processing. All processing was done using Bruker TopSpin 3.1 software.

Structure calculations

Solution structures were calculated using the Discover module (version 2000) of InsightII (Accelyrs, San Diego, CA) from ROESY cross-peaks as described previously (Chandrappa et al. 2012). NOE restraints obtained from ROESY spectra were categorized into three groups: strong (2.5 Å upper limit), medium (3.5 Å upper limit), and weak (5.0 Å upper limit) and structure calculations were carried out by restrained dynamics simulations using simulated annealing protocol. The resulting structures were analysed with Pymol (The PyMOL Molecular Graphics System, version 1.2r1, Schrödinger, LLC). A total of 27 NOEs, and 6 dihedral angles were used as constraints in the structure calculation.

X-ray diffraction

Diffraction quality single crystals of the peptide **1** were obtained by slow evaporation from the mixture of methanol and water. The X-ray diffraction dataset for the dodecapeptide was collected using MoK_{α} (0.71073 Å) radiation, on a BRUKER AXS KAPPA APEXII CCD diffractometer. Data collection was carried out in phi and omega scan type mode using dry crystals at 220 K. Peptide **1** crystals were

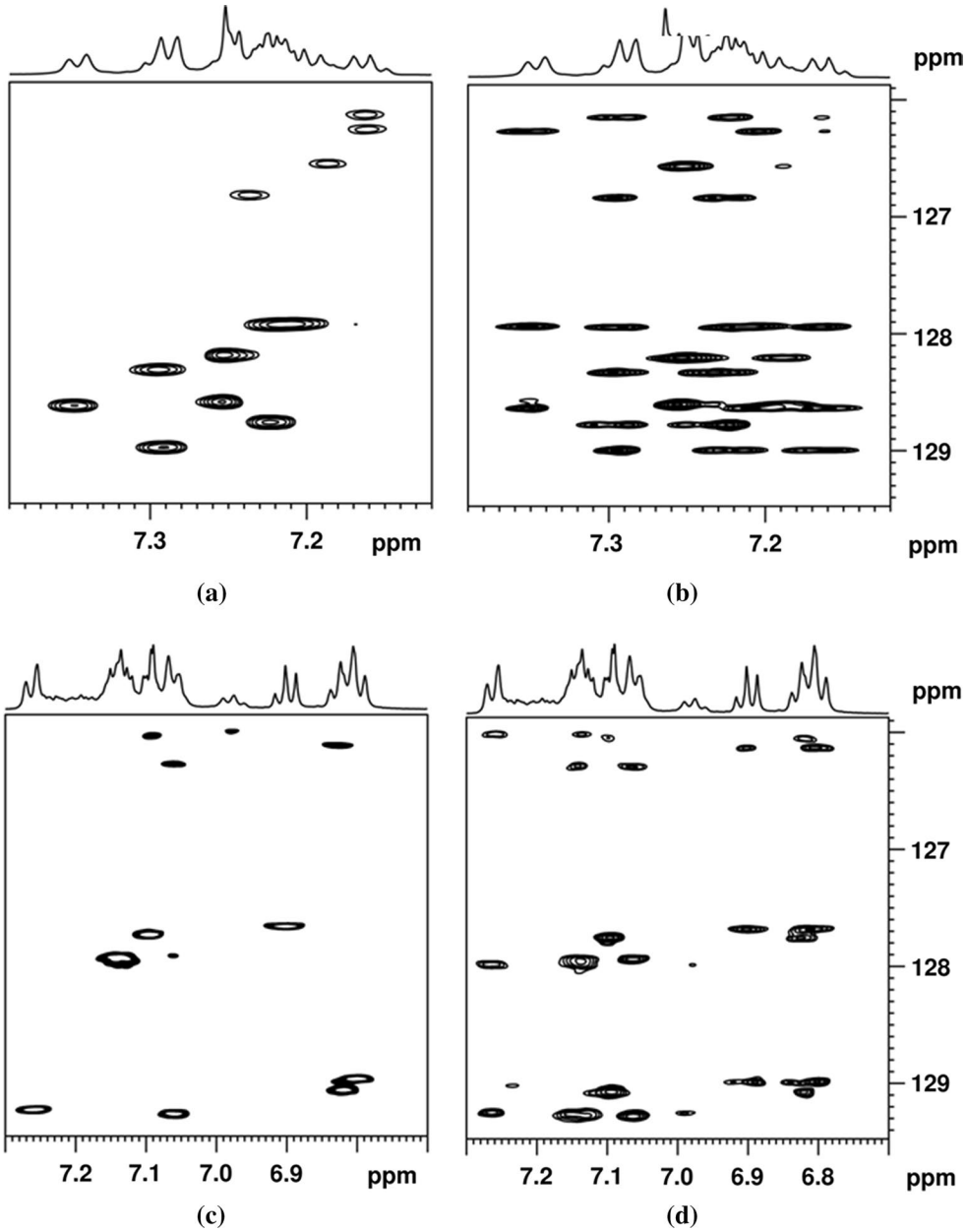

Fig. 8 Partial HSQC and HSQC-TOCSY spectra, illustrating the aromatic proton and carbon resonances of the peptides **1** and **2**, in CD_3OH. HSQC and HSQC-TOCSY spectra of peptide **1** is illustrated in (**a** and **b**), respectively. HSQC and HSQC-TOCSY spectra of peptide **2** are illustrated in (**c** and **d**), respectively

Table 5 Aromatic proton chemical shifts (ppm) of peptides in CD_3OH solution

Residue	H^{δ}		H^{ε}		H^{ζ}		$^{3}J_{C^{\alpha}H-C^{\beta}H}$ (Hz)	
	1	**2**	**1**	**2**	**1**	**2**	**1**	**2**
Phe(2)	7.22	7.06	7.29	7.14	7.24	7.06	7.80, 7.10	11.00, 5.40
Phe(4)	7.25	7.26	7.25	7.14	7.19	6.98	5.30, 10.30	9.20, 4.50
Phe(9)	7.35	6.80	7.20	6.90	7.16	6.83	3.00, 11.00	7.00, 6.30
Phe(11)	7.29	6.82	7.22	7.10	7.16	7.09	4.50, 9.80	10.00, 3.60

assigned to the orthorhombic space group $P2_12_12_1$ from systematic absences (h00, h = odd, 0k0, k = odd, 00l, l = odd). One peptide molecule and six co-crystallized solvent molecules (four methanol and two water molecules) constitute the crystallographic asymmetric unit. Crystal and diffraction parameters are listed in Table 2. The structure of the dodecapeptide was solved by using iterative dual-space direct methods using SHELXD (Schneider and Sheldrick 2002), which combines 'peak list optimization' (Sheldrick and Gould 1995) with the 'minimal function' involving

dual-space recycling. 1,214 large E values ($E > 1.2$) were used to obtain the structure solution from random phases, followed by peak list optimization. The final correlation coefficient (Fujinaga and Read 1987) was 83.85 %, suggesting a good initial model for refinement, with six fragments, consist of 95, 1, 1, 1, 1 and 1 atom. The remaining non-hydrogen atoms were located from difference Fourier maps. Isotropic refinement of the structure was carried out against F^2 followed by full matrix anisotropic least-squares refinement using SHELXL (Sheldrick 1997, 2008). The solvent molecules were located from difference Fourier maps. All hydrogen atoms attached to C atoms were fixed geometrically, in idealized positions, and allowed to ride with the respective C atoms to which each was bonded, in the final cycles of refinement. Hydrogen atoms attached to N atoms were located from difference Fourier maps and suitable restrained on N–H bond distances were applied with dfix command in order to get a chemically meaningful geometry. Apart from these, some other soft restraints on the C–O bond length of the solvent molecules were also applied. The final R-factor obtained was 0.0994 ($wR_2 = 0.3051$) for 9,673 observed reflections with $|F_o| > 4\sigma(F)$. The function minimized during the final refinement was $\sum w(|F_o|-F|)^2$, $w = 1/[\sigma^2 \times (F_o^2) + (0.168\ 6 \times P)^2 + 5.6991 \times P]$ where $P = [\max (F_o^2, 0) + 2F_c^2]/3$. The details of the crystal data and structure refinement parameters are listed in Table 2. Crystallographic information file has been deposited in the Cambridge Crystallographic Data Centre and may be obtained using the CCDC number 970559, via http://www.ccdc.cam.ac.uk/data_request/cif.

Conflict of interest We declare that we have no competing financial interests.

References

Altunbas A, Lee SJ, Rajasekaran SA, Schneider JP, Pochan DJ (2011) Encapsulation of curcumin in self-assembling peptide hydrogels as injectable drug delivery vehicles. Biomaterials 32:5906–5914

Aravinda S, Datta S, Shamala N, Balaram P (2004) Hydrogen-bond lengths in polypeptide helices: no evidence for short hydrogen bonds. Angew Chem Int Ed Engl 43:6728–6731

Aravinda S, Raghavender US, Rai R, Harini VV, Shamala N, Balaram P (2013a) Analysis of designed β-hairpin peptides: molecular conformation and packing in crystals. Org Biomol Chem 11:4220–4231

Aravinda S, Shamala N, Balaram P (2013b) In biomolecular forms and functions: a celebration of 50 years of the Ramachandran Map. In: Bansal M, Srinivasan N (eds). IISc Press-WSPC Publication, Bangalore, pp 264–281

Awasthi SK, Raghothama S, Balaram P (1995) A designed β-hairpin peptide. Biochem Biophys Res Commun 216:375–381

Benedetti E, Bavoso A, Di Blasio B, Pavone V, Pedone C, Crisma M, Bonora GM, Toniolo C (1982) Linear oligopeptides. 81. Solid-state and solution conformation of homooligo(α-aminoisobutyric acids) from tripeptide to pentapeptide: evidence for a 3_{10} helix. J Am Chem Soc 104:2437–2444

Bothner-By AA, Stephens RL, Lee J, Warren CD, Jeanloz RW (1984) Structure determination of a tetrasaccharide: transient nuclear Overhauser effects in the rotating frame. J Am Chem Soc 106:811–813

Braunschweiler L, Ernst RR (1983) Coherence transfer by isotropic mixing: application to proton correlation spectroscopy. J Magn Reson 53:521–528

Chandrappa S, Aravinda S, Raghothama S, Sonti R, Rai R, Harini VV, Shamala N, Balaram P (2012) Helix and hairpin nucleation in short peptides using centrally positioned conformationally constrained dipeptide segments. Org Biomol Chem 10:2815–2823

Crisma M, Formaggio F, Moretto A, Toniolo C (2006) Peptide helices based on α-amino acids. Biopolymers (Pept Sci) 84:3–12

Fujinaga M, Read RJ (1987) Experiences with a new translation-function program. J Appl Cryst 20:517–521

Gellman SH (1998) Minimal model systems for β-sheet secondary structure in proteins. Curr Opin Chem Biol 2:717–725

Gungormus M, Branco M, Fong H, Schneider JP, Tamerler C, Sarikaya M (2010) Self assembled bi-functional peptide hydrogels with biomineralization-directing peptides. Biomaterials 31:7266–7274

Haque TS, Little JC, Gellman SH (1996) Stereochemical requirements for β-hairpin formation: model studies with four-residue peptides and depsipeptides. J Am Chem Soc 118:6975–6985

Hwang TL, Shaka AJ (1995) Water suppression that works. excitation sculpting using arbitrary wave-forms and pulsed-field gradients. J Magn Reson Ser A 112:275–279

Karle IL, Balaram P (1990) Structural characteristics of.alpha-helical peptide molecules containing Aib residues. Biochemistry 29:6747–6756

Karle IL, Awasthi SK, Balaram P (1996) A designed beta-hairpin peptide in crystals. Proc Natl Acad Sci USA 93:8189–8193

Kay L, Keifer P, Saarinen T (1992) Pure absorption gradient enhanced heteronuclear single quantum correlation spectroscopy with improved sensitivity. J Am Chem Soc 114:10663–10665

Otting G, Wüthrich K (1988) Efficient purging scheme for proton-detected heteronuclear two-dimensional NMR. J Magn Reson 76:569–574

Prasad BVV, Balaram P (1984) The stereochemistry of peptides containing alpha-aminoisobutyric acid. CRC Crit Rev Biochem 16:307–348

Rai R, Raghothama S, Balaram P (2006) Design of a peptide hairpin containing a central three-residue loop. J Am Chem Soc 128:2675–2681

Rai R, Raghothama S, Sridharan R, Balaram P (2007) Tuning the β-turn segment in designed peptide β-hairpins: construction of a stable type I′ β-turn nucleus and hairpin–helix transition promoting segments. Biopolymers 88:350–361

Rajagopal K, Lamm MS, Haines-Butterick LA, Pochan DJ, Schneider JP (2009) Tuning the pH responsiveness of beta-hairpin peptide folding, self-assembly, and hydrogel material formation. Biomacromolecules 10:2619–2625

Rajagopal A, Aravinda S, Raghothama S, Shamala N, Balaram P (2011) Chain length effects on helix-hairpin distribution in short peptides with Aib-DAla and Aib-Aib Segments. Biopolymers 96:744–756

Rajagopal A, Aravinda S, Raghothama S, Shamala N, Balaram P (2012) Aromatic interactions in model peptide β-hairpins: ring current effects on proton chemical shifts. Biopolymers 98:185–194

Riedel T, Ghasparian A, Moehle K, Rusert P, Trkola A, Robinson JA (2011) Synthetic virus-like particles and conformationally constrained peptidomimetics in vaccine design. Chem Bio Chem 12:2829–2836

Robinson JA (2000) The design, synthesis and conformation of some new β-hairpin mimetics: novel reagents for drug and vaccine discovery. Synlett 2000:429–441

Robinson JA (2008) β-hairpin peptidomimetics: design, structures and biological activities. Acc Chem Res 41:1278–1288

Robinson JA (2013) Max Bergmann lecture Protein epitope mimetics in the age of structural vaccinology. J Pept Sci 19:127–140

Rughani RV, Schneider JP (2008) Molecular design of β-hairpin peptides for material construction. MRS Bull 33:530–535

Schmidt J, Patora-Komisarska K, Moehle K, Obrecht D, Robinson JA (2013) Structural studies of β-hairpin peptidomimetic antibiotics that target LptD in Pseudomonas. sp. Bioorg Med Chem 21:5806–5810

Schneider TR, Sheldrick GM (2002) Substructure solution with SHELXD. Acta Crystallogr D58:1772–1779

Sheldrick GM (1997) SHELXL-97, a program for crystal structure refinement. University of Göttingen, Göttingen

Sheldrick GM (2008) A short history of SHELX. Acta Cryst A64:112–122

Sheldrick GM, Gould RO (1995) Structure solution by iterative peaklist optimization and tangent expansion in space group P1. Acta Crystallogr B51:423–431

Sonti R, Rai R, Ragothama S, Balaram P (2012) NMR analysis of cross strand aromatic interactions in an 8 residue hairpin and a 14 residue three stranded β-sheet peptide. J Phys Chem B 116:14207–14215

Sonti R, Gopi HN, Muddegowda U, Ragothama S, Balaram P (2013) A designed three-stranded β-sheet in an α/β hybrid peptide. Chem Eur J 19:5955–5965

The PyMOL Molecular Graphics System, version 1.2r1. Schrödinger, LLC

Toniolo C, Benedetti E (1991) The polypeptide 3_{10}-helix. Trends Biochem Sci 16:350–353

Toniolo C, Bonora GM, Bavoso A, Benedetti E, Di Blasio B, Pavone V, Pedone C (1983) Preferred conformations of peptides containing α, α-disubstituted α-amino acids. Biopolymers 22:205–215

Veiga AS, Sinthuvanich C, Gaspar D, Franquelim HG, Castanho MARB, Schneider JP (2012) Arginine-rich self-assembling peptides as potent antibacterial gels. Biomaterials 33:8907–8916

Venkatraman J, Shankaramma SC, Balaram P (2001) Design of folded peptides. Chem Rev 101:3131–3152